Saudi Pharmaceutical Journal 25 (2017) 548–555

Contents lists available at ScienceDirect

Saudi Pharmaceutical Journal

journal homepage: www.sciencedirect.com

Original article

The first multiplication atom-bond connectivity index of molecular structures in drugs

Wei Gao [a,*], Yiqiao Wang [b], Weifan Wang [c], Li Shi [d]

[a] School of Information Science and Technology, Yunnan Normal University, Kunming 650500, China
[b] School of Management, Beijing University of Chinese Medicine, Beijing 100029, China
[c] Department of Mathematics, Zhejiang Normal University, Jinhua 321004, China
[d] Institute of Medical Biology, Chinese Academy of Medical Sciences & Peking Union Medical College, Kunming 650092, China

ARTICLE INFO

Article history:
Available online 28 April 2017

Keywords:
Theoretical medicine
Molecular graph
Multiplicative atom-bond connectivity index
Dendrimer

ABSTRACT

In the field of medicine, there are a large number of new drugs synthesis every year. Before entering the clinical stage, it needs a lot of work on drug testing of the various properties. Due to the lack of a large number of laboratory technician, laboratory equipment and reagents, the drug testing of many biochemical properties are not completed. Theoretical medicine provides a theoretical way for medical researchers to obtain the pharmaceutical properties of compounds by calculation tricks. In this paper, the first multiplication atom-bond connectivity index of several common drugs structure are studied, and the accurate expressions are determined. These theoretical conclusions provide practical guiding significance for pharmaceutical engineering.

1. Introduction

The increasing emergence of disease and the more and more mature medicine technology stimulate the development of newly invented drugs every year. As a result, it proposed the need to determine the pharmacological, chemical and biological features of these new drugs in experiments (Halim and Phang, 2017). On the other hand, it also threw us the tough work and make the relevant research much more headache. To be detailed, qualified and adequate reagents equipment and assisted researchers are necessary in the measurement for the performances and the side effects of the existing drugs (Mustafa et al., 2017). However, the equipment for the measurement of the biochemical properties is a tough problem in poor areas like some parts in South America, Africa and Southeast Asia. What should be glad is that the connection between chemical and pharmacodynamics characteristics of drugs and their molecular structures is found by researchers before (Feng et al., 2016; Xie et al., 2016; Tao et al., 2016). Concerning the definition of the topological indices, the indicators of these drug molecular structures are calculated. As a result, it's turned out to be efficient to make clear the medicinal properties and it can guarantee the well going of medicine and chemical experiments. In other word, the methods on topological index computation can help to get the available biological and medical information of new drugs without the support of chemical experiment hardware (Liu et al., 2016; Iftakhar et al., 2015; Sarfraz et al., 2016). Consequently, it is proved to be suitable to be used in poor parts of the world.

In the below, let $G = (V(G), E(G))$ be a molecular graph with vertex set $V(G)$ and edge set $E(G)$, then we can look upon a topological index as a map f: $G \to \mathbb{R}^+$. Several degree-based or distance-based indices like Randic index, Wiener index, harmonic index, PI index, sum connectivity index and others are borrowed here. Moreover, there are some mention-able contributions on distance-based and degree-based indices of special molecular structures and they can be referred to Harishchandra and Ramane (2016), Gao et al. (2016a,b,c,d), Gao et al. (2017a), Gao and Siddiqui (2017), Gao and Wang (2015, 2016) and Gao et al. (2017b).

The atom-bond connectivity index (shortly, *ABC* index) is defined by Estrada et al. (1998) as

$$ABC_1(G) = \sum_{uv \in E(G)} \sqrt{\frac{d(u) + d(v) - 2}{d(u)d(v)}}.$$

* Corresponding author.
E-mail address: gaowei@ynnu.edu.cn (W. Gao).

Peer review under responsibility of King Saud University.

Production and hosting by Elsevier

http://dx.doi.org/10.1016/j.jsps.2017.04.021

Very recently, Kulli (2016) defined the first multiplicative atom-bond connectivity index which stated as

$$ABC_1\mathrm{II}(G) = \prod_{uv\in E(G)} \sqrt{\frac{d(u)+d(v)-2}{d(u)d(v)}}.$$

Many papers contributed to different kinds of atom-bond connectivity indices. Farahani (2013a,b) determined the fourth atom-bond connectivity index of circumcoronene series of benzenoid. Goubko et al. (2015) presented an example to show the contradiction on the main result of previous work. Ahmadi and Sadeghimehr (2010) computed the atom bond connectivity index of some graphs and an infinite class of nanostar dendrimers. Husin et al. (2013) obtained the atom bond connectivity index of two families of nanostar dendrimers. Dehghan-Zadeh and Ashrafi (2014) studied the atom-bond connectivity index of quasi-tree graphs. Dehghan-Zadeh et al. (2014) determined the upper bound of atom-bond connectivity index in the class of tetracyclic graphs. Farahani (2013a,b) yielded the fourth atom-bond connectivity index of V-phenylenic nanotubes and nanotori. Dimitrov (2013) researched the efficient computation trick of trees with smallest atom-bond connectivity index. Ashrafi et al. (2015) raised the upper bound of atom-bond connectivity index of cactus graphs with fixed vertex number. Das et al. (2012) established the Upper bounds and Nordhaus-Gaddum type results for atom bond connectivity index.

The past forty years have witnessed the prosperity of the research on computation of degree-based and distance-based indices for certain special drug molecular structure. Despite the disagreements and conflicts on index computation of molecular graphs, the relevant research has made great progresses, but still leaving space for us to keep forward. Moreover, as widespread and critical drug structures, the applications of alkene, cycloalkenes, dendrimers, benzenoid systems and phenylenes are frequently found in chemical, medical, biological and pharmaceutical engineering. Therefore, a further discussion is needed to calculate the drug structures (Chen et al., 2016; Nawaz et al., 2017; Rashid et al., 2017).

The main contribution in this work is threefold: (1) the first multiplicative atom-bond connectivity index of alkene and cycloalkenes is obtained; (2) the expressions of the first multiplicative atom-bond connectivity index of special dendrimers are raised; (3) the formula of the first multiplicative atom-bond connectivity index of benzenoid systems and phenylenes is also obtained and analyzed.

2. Main results and proofs

In the below, the minimum and maximum degree of G are denoted by $\delta(G)$ and $\Delta(G)$. Edge set $E(G)$ and vertex set $V(G)$ are categorized into the following items:

- for any i with $\delta(G) \leqslant i \leqslant \Delta(G)$, let $D_i = \{u \in V(G) | d(v) = i\}$ and $d_i = |D_i|$
- for any i, j satisfy $\delta(G) lesi$, $j \leqslant \Delta(G)$, let $E_{i,j} = \{e = uv \in E(G) | d(u) = i,$ and $d(v) = j\}$ and $n_{ij} = |E_{i,j}|$.

2.1. The first multiplicative atom-bond connectivity index of alkene and cycloalkenes

In this part, we discuss the structure on alkene and cycloalkenes which are widely used in medicine and pharmaceutical engineering. Some applications on alkene and cycloalkenes can refer to Dziechciejewski et al. (2015), Babaee et al. (2012), Sysoiev et al. (2012), Tsarev et al. (2010), and Wilson et al. (2007).

As an unsaturated hydrocarbon with at least one carbon-carbon double bond, an alkene is composed of two hydrogen atoms less than the relevant alkane which has the same number of carbon atoms, with general formula C_nH_{2n}. The smallest alkene is ethylene (C_2H_4). Only a dobell bond between any two atoms of carbon is used to build the multiplicative ABC index for alkene, and in the

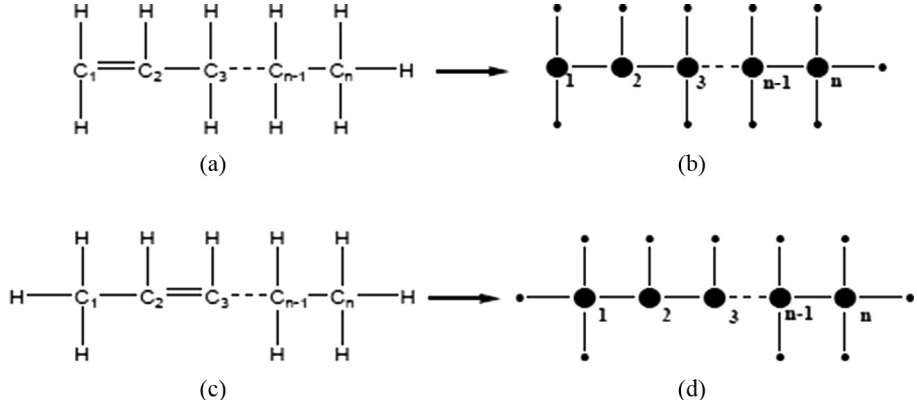

Fig. 1. (a) and (c) denote the molecular structure of alkenes C_nH_{2n}; (b) and (d) denote the molecular graph associated with chemical compound of alkenes C_nH_{2n}.

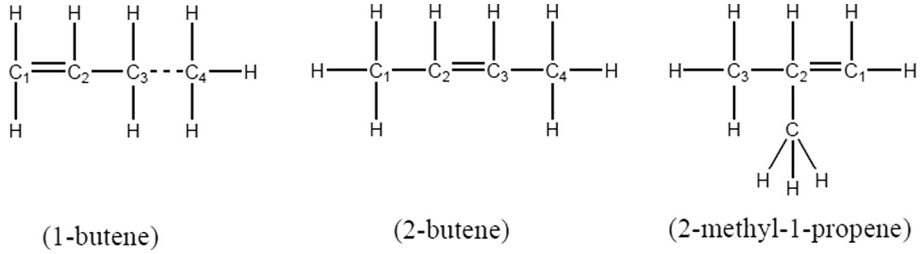

Fig. 2. Molecular structure of butene and methylpropene.

index the numbers of covalent bonds are 4 for carbon and 1 for hydrogen (see Fig. 1).

Theorem 1. *Let $n \geqslant 3$ be an integer. The first multiplicative atom-bond connectivity index of molecular structure in Fig. 1 associated with alkenes C_nH_{2n} is*

$$ABC_1\mathrm{II}(G) = \begin{cases} \frac{2}{3}\sqrt{\frac{5}{12}}\left(\sqrt{\frac{2}{3}}\right)^3\left(\frac{\sqrt{6}}{4}\right)^{n-3}\left(\frac{\sqrt{3}}{2}\right)^{2n-3}, \text{ if } n \geqslant 3 \text{ and } G = b \\ \frac{2}{3}\left(\sqrt{\frac{5}{12}}\right)^2\left(\sqrt{\frac{2}{3}}\right)^2\left(\frac{\sqrt{6}}{4}\right)^{n-4}\left(\frac{\sqrt{3}}{2}\right)^{2n-2}, \text{ if } n \geqslant 4 \text{ and } G = d \end{cases}.$$

Proof of Theorem 1. We present its proof by using mathematical induction and considering the following two cases.

- The molecular structure is described as Fig. 1(b).

If $n = 3$, then the molecular structure is associated with alkene C_3H_6 and its first multiplicative atom-bond connectivity index is

$$ABC_1II(G) = \sqrt{\frac{3+3-2}{3\cdot 3}} \times \sqrt{\frac{3+4-2}{3\cdot 4}}\left(\sqrt{\frac{3+1-2}{1\cdot 3}}\right)^3\left(\sqrt{\frac{4+1-2}{1\cdot 4}}\right)^3.$$

Thus, the result is true when $n = 3$. We assume that the results is correct for $n = k$, i.e., the first multiplicative atom-bond connectivity index of the molecular structure G associated with alkene C_kH_{2k} is

$$ABC_1\mathrm{II}(G) = \frac{2}{3}\sqrt{\frac{5}{12}}\left(\sqrt{\frac{2}{3}}\right)^3\left(\frac{\sqrt{6}}{4}\right)^{k-3}\left(\frac{\sqrt{3}}{2}\right)^{2k-3}.$$

Let C_i be the carbon vertex at the i-th position and e be the edge incident vertex k of this molecular structure with vertex corresponding to the end hydrogen vertex. Furterhmore, let G_1 be the molecular structure obtained from G by deleting the edge e, and G_2 be the molecular structure yielded by connecting the k-th vertex in G_1 with the center vertex of $K_{1,3}$. Hence, G_2 is the molecular structure G associated with alkene $C_{k+1}H_{2k+2}$, and

$$\begin{aligned} ABC_1II(G_2) &= \frac{ABC_1II(G)}{\sqrt{\frac{4+1-2}{4}}}\left(\sqrt{\frac{4+1-2}{4}}\right)^3\sqrt{\frac{4+4-2}{16}} \\ &= \frac{2}{3}\sqrt{\frac{5}{12}}\left(\sqrt{\frac{2}{3}}\right)^3\left(\frac{\sqrt{6}}{4}\right)^{k-3}\left(\frac{\sqrt{3}}{2}\right)^{2k-3} \times \left(\sqrt{\frac{4+1-2}{4}}\right)^2 \\ &\quad \times \sqrt{\frac{4+4-2}{16}} \\ &= \frac{2}{3}\sqrt{\frac{5}{12}}\left(\sqrt{\frac{2}{3}}\right)^3\left(\frac{\sqrt{6}}{4}\right)^{k-2}\left(\frac{\sqrt{3}}{2}\right)^{2k-1}. \end{aligned}$$

Thus, the result is correct when $n = k + 1$.

- The molecular structure is described in Fig. 1(d).

We can deduce the desired conclusion in terms of the tricks presented in the above case.

All the alkenes that own 4 or more carbon atoms display structural isomerism. Even though there are lots in common among structural isomers, they share different structural formulas. Therefore, one molecular formula could be drawn from the different structural formulas. To illustrate, the following two

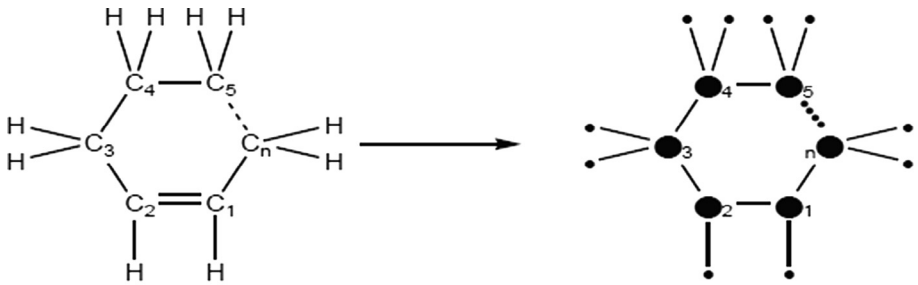

Fig. 3. (a) Structure of cycloalkenes C_n^H and its molecular graph expression.

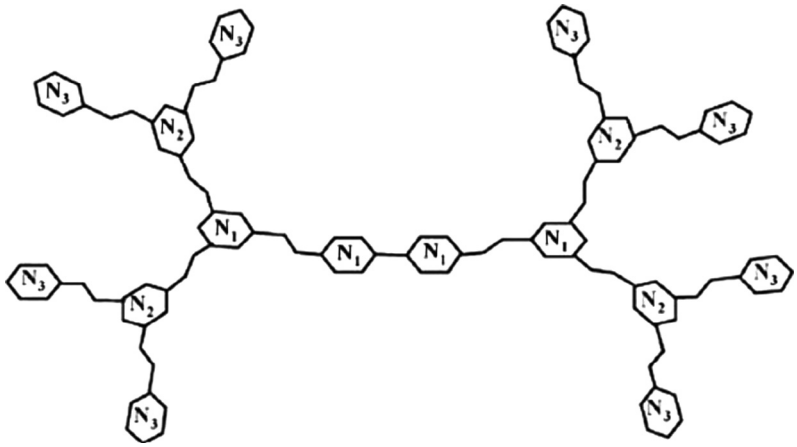

Fig. 4. The basic molecular structure of $NS_2[n]$.

different molecules can share the same formula C_4H_8. These can be named 1-butene and 2-methylpropene respectively (see Fig. 2). □

Structural isomers share the common molecular formula but different structural expression, so that the multiplicative atom bond connectivity index of isomers of alkenes shares the same general formula in Theorem 1 (Safi et al., 2015; Razali and Said, 2017). As a result, the same numbers of carbon and hydrogen atoms are also the same in isomers of alkenes and the same degree of vertices are in the same number of edges.

Cycloalkenes (also called a cycloolefin) is a type of alkene hydrocarbon with a closed ring of carbon atoms. The Greek prefix cyclo- represents round here. If the ends of a carbon chain are connected one with one, the molecule becomes cyclic or round, and then there is no difference between alkenes and other carbon chains (see Fig. 3).

Theorem 2. *Let $n \geqslant 3$ be an integer. The first multiplicative atom-bond connectivity index of molecular structure in Fig. 3(b) associated with alkenes C_n^H is*

$$ABC_1\mathrm{II}(G) = \frac{2}{3}\left(\sqrt{\frac{5}{12}}\right)^2\left(\sqrt{\frac{2}{3}}\right)^2\left(\frac{\sqrt{3}}{2}\right)^{2n-4}\left(\frac{\sqrt{6}}{4}\right)^{n-3}.$$

Proof of Theorem 2. We present its proof by using mathematical induction. Let G_n be the molelcular strcture associated with C_n^H.

If $n = 3$, then the molecular structure is associated with alkene C_3^H and its first multiplicative atom-bond connectivity index is

$$ABC_1\mathrm{II}(G_3) = \frac{2}{3}\left(\sqrt{\frac{5}{12}}\right)^2\left(\sqrt{\frac{2}{3}}\right)^2\left(\frac{\sqrt{3}}{2}\right)^2.$$

Thus, the result is true when $n = 3$. We assume that the results are correct for $n = k$, i.e., the first multiplicative atom-bond connectivity index of the molecular structure G_k associated with alkene C_k^H is

$$ABC_1II(G_k) = \frac{2}{3}\left(\sqrt{\frac{5}{12}}\right)^2\left(\sqrt{\frac{2}{3}}\right)^2\left(\frac{\sqrt{3}}{2}\right)^{2k-4}\left(\frac{\sqrt{6}}{4}\right)^{k-3}.$$

Let e be the edge connecting the 1-th vertex with k-th vertex, G' be the molecular structure obtained from G_k by deleting the edge e, and G'' be the molecular structure yielded by connecting G' and $K_{1,4}$ (with x_1 has degree 4, $x_2 \sim x_5$ has degree 1) using the following way:

x_1 = k+1-th vertex in G'; x_2 = 1-th vertex in G'; x_3 = k-th vertex in G'.

Hence, G'' is the molecular structure G_{k+1} associated with alkene C_{k+1}^H, and

$$\begin{aligned}ABC_1\mathrm{II}(G_{k+1}) &= \frac{ABC_1II(G_k)}{\sqrt{\frac{4+3-2}{12}}}\sqrt{\frac{4+3-2}{12}}\sqrt{\frac{4+4-2}{16}}\left(\sqrt{\frac{1+4-2}{4}}\right)^2\\ &= \frac{2}{3}\left(\sqrt{\frac{5}{12}}\right)^2\left(\sqrt{\frac{2}{3}}\right)^2\left(\frac{\sqrt{3}}{2}\right)^{2k-4}\left(\frac{\sqrt{6}}{4}\right)^{k-3}\\ &\quad\times\sqrt{\frac{4+4-2}{16}}\left(\sqrt{\frac{1+4-2}{4}}\right)^2\\ &= \frac{2}{3}\left(\sqrt{\frac{5}{12}}\right)^2\left(\sqrt{\frac{2}{3}}\right)^2\left(\frac{\sqrt{3}}{2}\right)^{2k-2}\left(\frac{\sqrt{6}}{4}\right)^{k-2}.\end{aligned}$$

Thus, the result is correct when $n = k + 1$. □

2.2. The first multiplicative atom-bond connectivity index of dendrimers

In this subsection, we determine the first multiplicative atom-bond connectivity index of dendrimers which is widely appeared in the drug structures. More medicine engineering applications on different kinds of dendrimers can be referred in Cevik et al. (2016), Heredero-Bermejo et al. (2016, 2015), Worley et al. (2016), Vacas-Cordoba et al. (2016), Rivero-Buceta et al. (2015), Ozcan and Sezginturk (2015), Gothwal et al. (2015), and Sepulveda-Crespo et al. (2015). In Theorem 3–Theorem 6, we assume n be the growth stages.

Theorem 3. *The first multiplicative atom-bond connectivity index of nano-star $NS_2[n]$ is*

$$ABC_1\mathrm{II}(NS_2[n]) = \frac{2}{3}\left(\frac{\sqrt{2}}{2}\right)^{18\cdot 2^n-6}.$$

Proof of Theorem 3. The molecular structure of $NS_2[n]$ is stated in Fig. 4: By analyzing the structure of $NS_2[n]$,we ensure that the edge set $E(NS_2[n])$ can be divided into three partitions:

- $E_{2,2} = \{e = uv \in E(G)|d(u) = d(v) = 2\}$ and $n_{22} = 6 \cdot 2^n + 2$;
- $E_{2,3} = \{e = uv \in E(G)|d(u) = 2 \text{ and } d(v) = 3\}$ and $n_{23} = 12 \cdot 2^n - 8$;
- $E_{3,3} = \{e = uv \in E(G)|d(u) = d(v) = 3\}$ and $n_{33} = 1$.

Hence, by means of the definitions of first multiplicative atom-bond connectivity index, we get the desired result. □

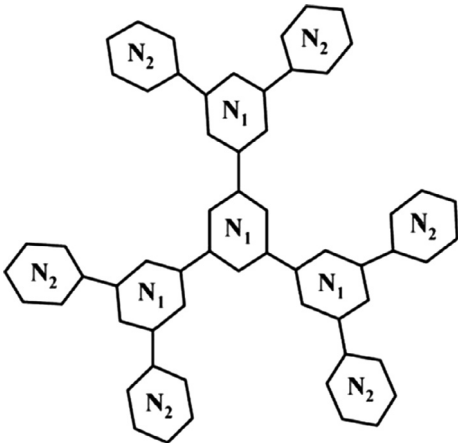

Fig. 5. The basic molecular structure of $NS_3[n]$.

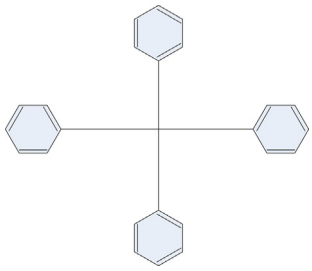

Fig. 6. The kernel of $D_4[n]$.

Theorem 4. *The first multiplicative atom-bond connectivity index of nano-star $NS_3[n]$ is*

$$ABC_1\mathrm{II}(NS_3[n]) = \left(\frac{2}{3}\right)^{3\cdot 2^n-3}\left(\frac{\sqrt{2}}{2}\right)^{18\cdot 2^n-12}.$$

Proof of Theorem 4. The molecular structure of $NS_3[n]$ is stated in Fig. 5. By analyzing the structure of $NS_3[n]$, we ensure that the edge set $E(NS_3[n])$ can be divided into three partitions:

- $E_{2,2} = \{e = uv \in E(G)|d(u) = d(v) = 2\}$ and $n_{22} = 6\cdot 2^n$;
- $E_{2,3} = \{e = uv \in E(G)|d(u) = 2$ and $d(v) = 3\}$ and $n_{23} = 12\cdot 2^n - 12$;
- $E_{3,3} = \{e = uv \in E(G)|d(u) = d(v) = 3\}$ and $n_{33} = 3\cdot 2^n - 3$.

Thus, in terms of the definitions of first multiplicative atom-bond connectivity index, we infer the desired result. □

Theorem 5. *The first multiplicative atom-bond connectivity index of polyphenylene dendrimer $D_4[n]$ is*

$$ABC_1\mathrm{II}(D_4[n]) = \left(\sqrt{\frac{5}{12}}\right)^4\left(\frac{2}{3}\right)^{36\cdot 2^n-36}\left(\frac{\sqrt{2}}{2}\right)^{104\cdot 2^n-80}.$$

Proof of Theorem 5. The kernel and an example of $D_4[n]$ are presented in Figs. 6 and 7, respectively. By analyzing the structure of $D_4[n]$, we ensure that the edge set $E(D_4[n])$ can be divided into four partitions:

- $E_{2,2} = \{e = uv \in E(G)|d(u) = d(v) = 2\}$ and $n_{22} = 56\cdot 2^n - 40$
- $E_{2,3} = \{e = uv \in E(G)|d(u) = 2$ and $d(v) = 3\}$ and $n_{23} = 48\cdot 2^n - 40$;
- $E_{3,3} = \{e = uv \in E(G)|d(u) = d(v) = 3\}$ and $n_{33} = 36\cdot 2^n - 36$;
- $E_{3,3} = \{e = uv \in E(G)|d(u) = 3$ and $d(v) = 4\}$ and $n_{34} = 4$.

Therefore, in light of the definitions of first multiplicative atom-bond connectivity index, we yield the result in Theorem 5. □

Theorem 6. *The first multiplicative atom-bond connectivity index of polyphenylene dendrimer $D_2[n]$ is*

$$ABC_1\mathrm{II}(D_2[n]) = \left(\frac{2}{3}\right)^{36\cdot 2^n-35}\left(\frac{\sqrt{2}}{2}\right)^{104\cdot 2^n-92}.$$

Proof of Theorem 6. The kernel and an example of $D_2[n]$ are presented in Figs. 8 and 9, respectively.By analyzing the structure of $D_2[n]$, we ensure that the edge set $E(D_2[n])$ can be divided into three partitions:

- $E_{2,2} = \{e = uv \in E(G)|d(u) = d(v) = 2\}$ and $n_{22} = 56\cdot 2^n - 48$;
- $E_{2,3} = \{e = uv \in E(G)|d(u) = 2$ and $d(v) = 3\}$ and $n_{23} = 48\cdot 2^n - 44$;
- $E_{3,3} = \{e = uv \in E(G)|d(u) = d(v) = 3\}$ and $n_{33} = 36\cdot 2^n - 35$.

Therefore, using the definitions of the first multiplicative atom-bond connectivity index, we deduce the result. □

Fig. 8. The kernel of $D_2[n]$.

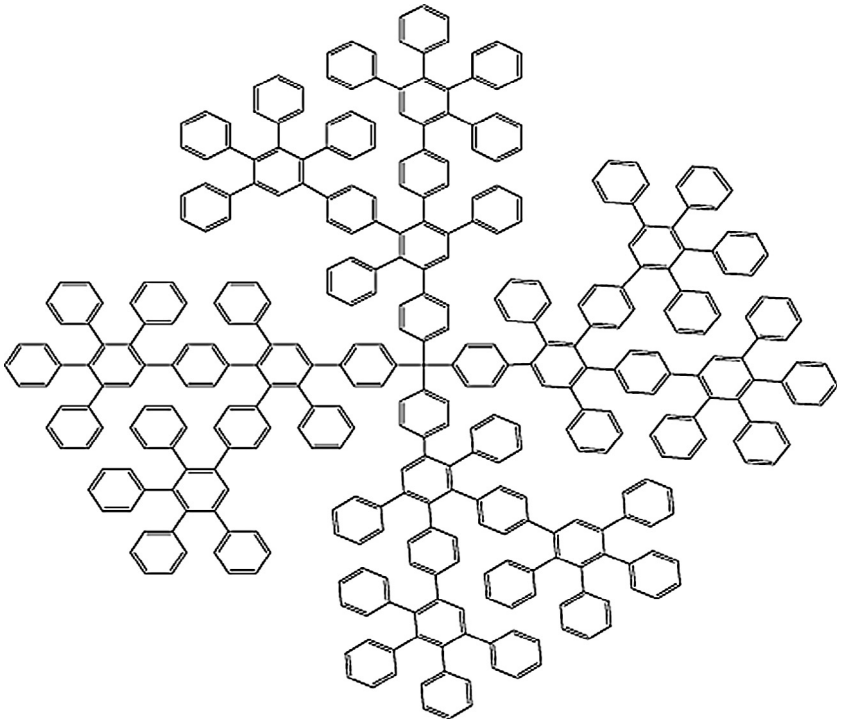

Fig. 7. The molecular struture of $D_4[n]$ with 2 growth stages.

2.3. The first multiplicative atom-bond connectivity index of benzenoid systems and phenylenes

First, we introduce some notations of benzenoid systems and phenylenes:

- r the number of inlets;
- B the number of simple bays;
- C the number of coves;
- F the number of fjords;
- f the number of fissures;
- L the number of lagoons;
- b the number of regions.

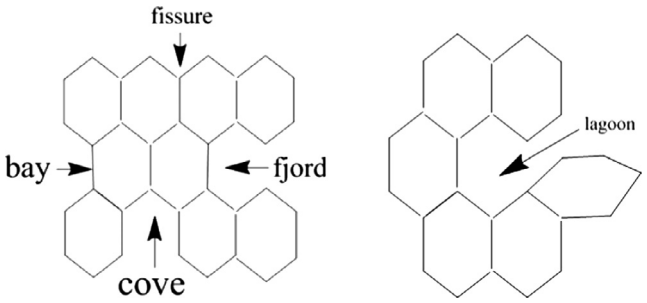

Fig. 10. Some kinds of inlets in the perimeter of a benzenoid system.

It's necessary to mention that bays, coves, fjords, fissures and lagoons are structural characteristics of the perimeter of the benzenoid systems and they are important in their theory. For the description of examples, please refer to Fig. 10.

Then if we assume r be the sum of inlets on the perimeters of a benzenoid system represented just now, we can obtain $b = B + 2C + 3F + 4L$ and $r = B + C + F + f + L$.

Phenylenes are a kind of chemical compounds and the carbon atoms form 6- and 4-membered cycles in it. Every 4-membered cycle(=square) is next to two disjoint 6-membered cycles(=hexagons), and no two hexagons are found to be next to each other. The hexagonal squeeze of the respective phenylene, a catacondensed hexagonal system (which may be jammed), is obtained by eliminating, and "squeezing out" the squares from a phenylene (Yine et al., 2015; Shareef et al., 2017). Obviously, a phenylene (PH) is corresponding to its hexagonal squeeze (HS), for they share the same number (h) of hexagons. Moreover, a phenylene with h hexagons own $h - 1$ squares. The number of vertices of pH and HS are $6h$ and $4h + 2$, respectively; The number of edges of pH and HS are $8h - 2$ and $5h + 1$, respectively. For description of the example of phenylene and its hexagonal squeeze, please refer to Fig. 11.

As for the example of phenylenes, a fissure, bay, cove, fjord, and lagoon are considered as the benzenoid systems. A fissure (resp. a bay, cove, fjord, or lagoon) is corresponding to a sequence of four (resp, six, eight, ten, and twelve) consecutive vertices on the perimeter, and the first and the last of it are 2 degree vertices and the rest are 3 degree vertices.

Several contributions and engineering applications on benzenoid systems and phenylenes can refer to Cruz et al. (2013), Dias (2010), Smirnova et al. (2017), Koyama et al. (2017), Nguyen et al. (2017), Abdulkarim et al. (2016), Rai et al. (2016), Selter et al. (2016), and Raju et al. (2016). Now, the main conclusions in this part are stated as follows.

Theorem 7. *The first multiplicative atom-bond connectivity index of benzenoid system S with n vertices, h hexagons and r inlets is*

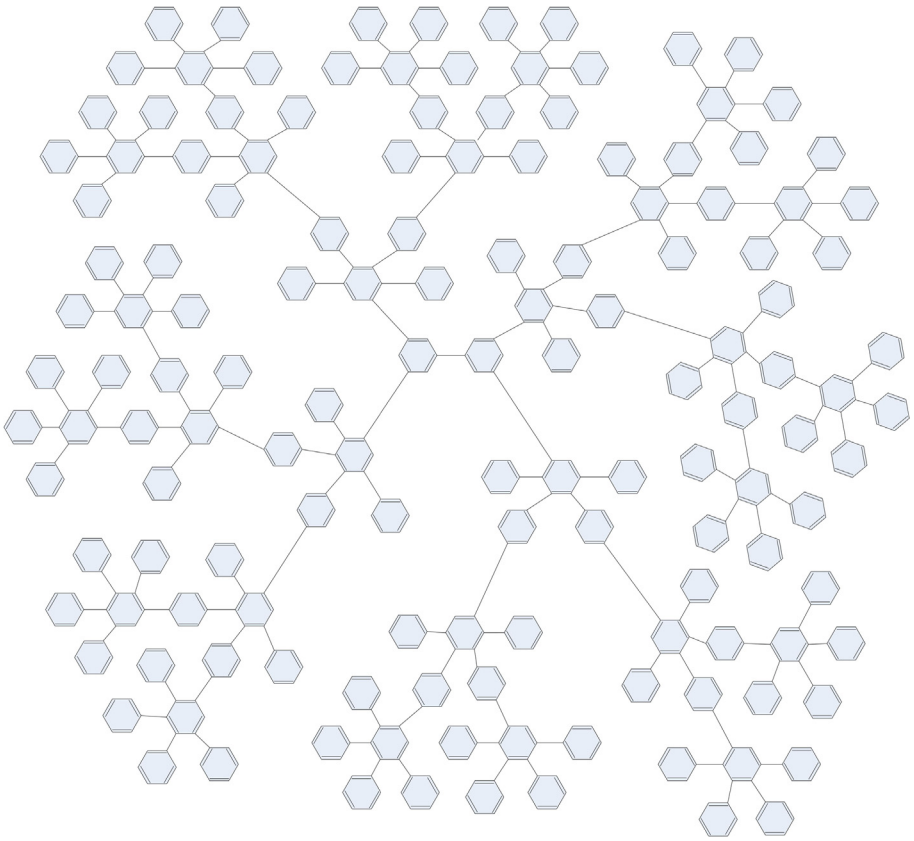

Fig. 9. The molecular struture of $D_2[n]$ with 3 growth stages.

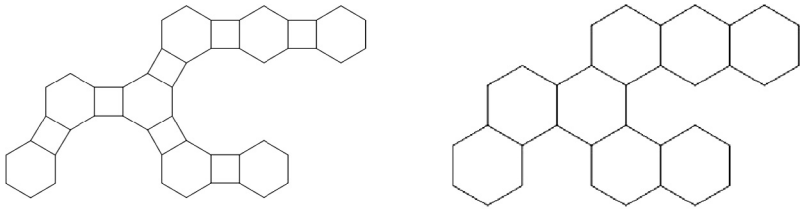

Fig. 11. A phenylene PH and its hexagonal squeeze HS.

$$ABC_1\mathrm{II}(S) = \left(\frac{2}{3}\right)^{3h-r-3}\left(\frac{\sqrt{2}}{2}\right)^{n-2h+r+2}.$$

Proof of Theorem 7. Clearly, the edge set $E(S)$ can be divided into three partitions:

- $E_{2,2} = \{e = uv \in E(G) | d(u) = d(v) = 2\}$ and $n_{22} = n - 2h - r + 2$;
- $E_{2,3} = \{e = uv \in E(G) | d(u) = 2$ and $d(v) = 3\}$ and $n_{23} = 2r$;
- $E_{3,3} = \{e = uv \in E(G) | d(u) = d(v) = 3\}$ and $n_{33} = 3h - r - 3$.

By simple calculation, we infer the desired result. □

Theorem 8. *The first multiplicative atom-bond connectivity index of phenylene PH with h hexagons and r inlets is*

$$ABC_1\mathrm{II}(PH) = \left(\frac{2}{3}\right)^{6h-r-6}\left(\frac{\sqrt{2}}{2}\right)^{2h+r+4}$$

Proof of Theorem 8. Obviously, the edge set $E(PH)$ can be divided into three partitions:

- $E_{2,2} = \{e = uv \in E(G) | d(u) = d(v) = 2\}$ and $n_{22} = 2h - r + 4$;
- $E_{2,3} = \{e = uv \in E(G) | d(u) = 2$ and $d(v) = 3\}$ and $n_{23} = 2r$;
- $E_{3,3} = \{e = uv \in E(G) | d(u) = d(v) = 3\}$ and $n_{33} = 6h - r - 6$.

By simple calculation, we infer the desired result. □

3. Conclusion

This paper proposed the multiplicative atom-bond connectivity index of alkene, cycloalkenes, dendrimers, benzenoid systems and phenylenes by analyzing certain molecular structural, degree computation and mathematical derivation. The conclusion also demonstrate the wide and promising application prospect in medical and pharmacy engineering.

Conflict of interests

The authors declare that there is no conflict of interests regarding the publication of this paper.

Acknowledgements

We thank the reviewers for their constructive comments in improving the quality of this paper. This work was supported in part by the National Natural Science Foundation of China (11401519).

References

Abdulkarim, A., Hinkel, F., Jansch, D., Freudenberg, J., Golling, F.E., Mullen, K., 2016. A new solution to an old problem: synthesis of unsubstituted poly (para-phenylene). J. Am. Chem. Soc. 138 (50), 16208–16211.
Ahmadi, M.B., Sadeghimehr, M., 2010. Atom bond connectivity index of an infinite class NS1[n] of dendrimer nanostars. Optoelectron. Adv. Mater.-Rapid Commun. 4 (7), 1040–1042.
Ashrafi, A.R., Dehghan-Zadeh, T., Habibi, N., 2015. Extremal atom-bond connectivity index of cactus graphs. Commun. Korean Math. Soc. 30 (3), 283–295.
Babaee, S., Hashemi, H., Javanmardi, J., Eslamimanesh, A., Mohammadi, A.H., 2012. Thermodynamic model for prediction of phase equilibria of clathrate hydrates of hydrogen with different alkanes, alkenes, alkynes, cycloalkanes or cycloalkene. Fluid Phase Equilib. 336, 71–78.
Cevik, E., Bahar, O., Senel, M., Abasiyanik, M.F., 2016. Construction of novel electrochemical immunosensor for detection of prostate specific antigen using ferrocene-PAMAM dendrimers. Biosens. Bioelectron. 86, 1074–1079.
Chen, Y., Gao, Y., Ashraf, M.A., Gao, W., 2016. Effects of the traditional chinese medicine dilong on airway remodeling in rats with OVA-induced-Asthma. Open Life Sci. 11 (1), 498–505.
Cruz, R., Gutman, I., Rada, J., 2013. On benzenoid systems with a minimal number of inlets. J. Serb. Chem. Soc. 78 (9), 1351–1357.
Das, K.C., Gutman, I., Furtula, B., 2012. On atom-bond connectivity index. Filomat 26 (4), 733–738.
Dehghan-Zadeh, T., Ashrafi, A.R., 2014. Atom–bond connectivity index of quasi-tree graphs. Rendicontidel Circolo Matematico di Palermo. 63, 347–354.
Dehghan-Zadeh, T., Ashrafi, A.R., Habibi, N., 2014. Maximum values of atom-bond connectivity index in the class of tetracyclic graphs. J. Appl. Math. Comput. 46, 285–303.
Dias, J.R., 2010. The polyhex/polypent topological paradigm: regularities in the isomer numbers and topological properties of select subclasses of benzenoid hydrocarbons and related systems. Chem. Soc. Rev. 39 (6), 1913–1924.
Dimitrov, D., 2013. Efficient computation of trees with minimal atom-bond connectivity index. Appl. Math. Comput. 224, 663–670.
Dziechciejewski, W.J., Weber, R., Sowada, O., Boysen, M.M.K., 2015. Cycloalkene carbonitriles in rhodium-catalyzed 1, 4-addition and formal synthesis of vabicaserin. Org. Lett. 17 (17), 4132–4135.
Estrada, E., Torres, L., Rodriguez, L., Gutman, I., 1998. An atombond connectivity index: modelling the enthalpy of formation of alkanes. Indian J. Chem. A 37 (10), 849–855.
Farahani, M.R., 2013a. Computing atom-bond connectivity (ABC4) index for circumcoronene series of benzenoid. J. Adv. Chem. 2 (1), 68–72.
Farahani, M.R., 2013b. Computing fourth atom-bond connectivity index of V-phenylenic nanotubes and nanotori. Acta Chim. Slov. 60 (2), 429–432.
Feng, B., Ashraf, M.A., Peng, L., 2016. Characterization of particle shape, zeta potential, loading efficiency and outdoor stability for chitosan-ricinoleic acid loaded with rotenone. Open Life Sci. 11 (1), 380–386.
Gao, W., Baig, A.Q., Ali, H., Sajjad, W., Farahani, M.R., 2017a. Margin based ontology sparse vector learning algorithm and applied in biology science. Saudi J. Biol. Sci. 24 (1), 132–138.
Gao, W., Farahani, M.R., Shi, L., 2016a. The forgotten topological index of some drug structures. Acta Med. Mediterranea 32, 579–585.
Gao, W., Siddiqui, M.K., 2017. Molecular descriptors of nanotube, oxide, silicate, and triangulene networks. J. Chem. Article ID 6540754, 10 pages, doi: http://dx.doi.org/10.1155/2017/6540754.
Gao, W., Siddiqui, M.K., Imran, M., Jamil, M.K., Farahani, M.R., 2016b. Forgotten topological index of chemical structure in drugs. Saudi Pharm. J. 24, 258–264.
Gao, W., Wang, W.F., 2015. The vertex version of weighted wiener number for bicyclic molecular structures. Comput. Math. Methods Med., Article ID 418106, 10 pages, doi: http://dx.doi.org/10.1155/2015/418106.
Gao, W., Wang, W.F., 2016. The eccentric connectivity polynomial of two classes of nanotubes. Chaos, Solitons Fractals 89, 290–294.
Gao, W., Wang, W.F., Farahani, M.R., 2016. Topological indices study of molecular structure in anticancer drugs. J. Chem., Article ID 3216327, 8 pages, doi: http://dx.doi.org/10.1155/2016/3216327.
Gao, W., Wang, W.F., Jamil, M.K., Farahani, M.R., 2016. Electron energy studying of molecular structures via forgotten topological index computation. J. Chem., Article ID 1053183, 7 pages, doi: http://dx.doi.org/10.1155/2016/1053183.

Gao, W., Yan, L., Shi, L., 2017b. Generalized Zagreb index of polyomino chains and nanotubes. Optoelectron. Adv. Mater.-Rapid Commun. 11 (1–2), 119–124.
Gothwal, A., Kesharwani, P., et al., 2015. Dendrimers as an effective nanocarrier in cardiovascular disease. Curr. Pharm. Des. 21 (30), 4519–4526.
Goubko, M., Magnant, C., Nowbandegani, P.S., Gutman, I., 2015. ABC index of trees with fixed number of leaves. MATCH Commun. Math. Comput. Chem. 74, 697–702.
Halim, A.N.I., Phang, I.C., 2017. Salicylic acid mitigates pb stress in Nicotiana tabacum. Galeri Warisan Sains 1 (1), 16–19.
Harishchandra, S., Ramane, R.B., 2016. Note on forgotten topological index of chemical structure in drugs. Appl. Math. Nonlinear Sci. 1 (2), 369–374.
Heredero-Bermejo, I., Copa-Patino, J.L., et al., 2015. Evaluation of the activity of new cationic carbosilane dendrimers on trophozoites and cysts of acanthamoeba polyphaga. Parasitol. Res. 114 (2), 473–486.
Heredero-Bermejo, I., Sanchez-Nieves, J., Soliveri, J., et al., 2016. In vitro anti-Acanthamoeba synergistic effect of chlorhexidine and cationic carbosilanedendrimers against both trophozoite and cyst forms. Int. J. Pharm. 509 (1–2), 1–7.
Husin, N.M., Hasni, R., Arif, N.E., 2013. Atom-bond connectivity and geometric arithmetic indices of dendrimer nanostars. Aust. J. Basic Appl. Sci. 7 (9), 10–14.
Iftakhar, A., Hasan, I.J., Sarfraz, M., Jafri, L., Ashraf, M.A., 2015. Nephroprotective effect of the leaves of Aloe barbadensis (Aloe Vera) against toxicity induced by diclofenac sodium in albino rabbits. West Indian Med. J. 64 (5), 462–467.
Koyama, H., Watanabe, Y., Suzuki, A., 2017. Preparation and mechanical properties of poly (p-phenylene sulfide) nanofiber sheets obtained by CO_2 laser supersonic multi-drawing. J. Polym. Eng. 37 (1), 53–60.
Kulli, V.R., 2016. Multiplicative connectivity indices of certain nanotubes. Ann. Pure Appl. Math. 12 (2), 169–176.
Liu, Z.K., Gao, P., Ashraf, M.A., Wen, J.B., 2016. The complete mitochondrial genomes of two weevils, *Eucryptorrhynchus chinensis* and *E. brandti*: conserved genome arrangement in Curculionidae and deficiency of tRNA-Ile gene. Open Life Sci. 11 (1), 458–469.
Mustafa, G., Arif1, R., Atta, A., Sharif, S., Jamil, A., 2017. Bioactive compounds from medicinal plants and their importance in drug discovery in Pakistan. Matrix Sci. Pharma 1 (1), 17–26.
Nawaz, S., Shareef, M., Shahid, H., Mushtaq, M., Sarfraz, M., 2017. A review of antihyperlipidemic effect of synthetic phenolic compounds. Matrix Sci. Med. 1 (1), 22–26.
Nguyen, T.K.L., Livi, S., et al., 2017. Toughening of epoxy/Ionic liquid networks with thermoplastics based on poly (2, 6-dimethy1-1,4-phenylene ether) (PPE). ACS Sustain. Chem. Eng. 5 (1), 1153–1164.
Ozcan, H.M., Sezginturk, M.K., 2015. Detection of parathyroid hormone using an electrochemical impedance biosensor based on PAMAM dendrimers. Biotechnol. Prog. 31 (3), 815–822.
Rai, S., Patel, P.N., Chadha, A., 2016. Preparation, characterisation, and crystal structure analysis of (2E, 2′E)-3, 3′-(1, 4-phenylene) bis (1-(2-aminophenyl) prop-2-en-1-one. Crystallogr. Rep. 61 (7), 1086–1089.
Raju, T.S., Vaghasiya, J.V., et al., 2016. Influence of m-fluorine substituted phenylene spacer dyes in dye-sensitized solar cells. Org. Electron. 39, 371–379.
Rashid, M., Saleem, M.I., Deeba, F., Khan, M.S., Mahfooz, S.A., Butt, A.A., Abbas, M.W., 2017. Effect of season on occurrence of caprine mastitis in beetal in faisalabad premises. Matrix Sci. Med. 1 (1), 19–21.
Razali, M.A.A., Said, F.M., 2017. Red pigment production by monascus purpureus in stirred-drum bioreactor. Galeri Warisan Sains 1 (1), 13–15.
Rivero-Buceta, E., Doyaguez, E.G., et al., 2015. Tryptophan dendrimers that inhibit HIV replication, prevent virus entry and bind to the HIV envelope glycoproteins gp120 and gp41. Eur. J. Med. Chem. 106, 34–43.
Safi, S.Z., Qvist, R., Chinna, K., Ashraf, M.A., Paramasivam, D., Ismail, I.S., 2015. Gene expression profiling of the peripheral blood mononuclear cells of offspring of one type 2 diabetic parent. Int. J. Diabetes Develop. Countries 2015, 1–8.
Sarfraz, M., Ashraf, Y., Sajid, S., Ashraf, M.A., 2016. Testosterone level in testicular cancer patients after chemotherapy. West Indian Med. J. 64 (5), 487–494.
Selter, P., Grote, S., Brunklaus, G., 2016. Synthesis and Li-7 ion dynamics in polyarylene-ethersulfone-phenylene-oxide-based polymer electrolytes. Macromol. Chem. Phys. 217 (23), 2584–2594.
Sepulveda-Crespo, D., Sanchez-Rodriguez, J., et al., 2015. Triple combination of carbosilane dendrimers, tenofovir and maraviroc as potential microbicide to prevent HIV-1 sexual transmission. Nanomedicine 10 (6), 899–914.
Shareef, M., Jamal, M., Sarfraz, M., 2017. A review of anti-bacterial activity of Nigella sativa in gut of broiler chicks. Matrix Sci. Pharma 1 (1), 27–32.
Smirnova, N.N., Samosudova, Y.S., et al., 2017. Thermodynamic properties of poly (phenylene-pyridyl) dendrons of second and the third generations. J. Chem. Thermodyn. 105, 443–451.
Sysoiev, D., Yushchenko, T., et al., 2012. Pronounced effects on switching efficiency of diarylcycloalkenes upon cycloalkene ring contraction. Chem. Commun. 48 (92), 11355–11357.
Tao, X., Ashraf, M.A., Zhao, Y., 2016. Paired observation on light-cured composite resin and nano-composite resin in dental caries repair. Pak. J. Pharm. Sci. 29 (6), 2169–2172.
Tsarev, V.N., Wolters, D., Gais, H.J., 2010. Redox reaction of the Pd-0 complex bearing the Trost ligand with meso-cycloalkene-1,4-biscarbonates leading to a diamidato Pd-II complex and 1,3-cycloalkadienes: enantioselective desymmetrization versus catalyst deactivation. Chem.-A Eur. J. 16 (9), 2904–2915.
Vacas-Cordoba, E., Maly, M., De la Mata, F.J., et al., 2016. Antiviral mechanism of polyanionic carbosilane dendrimers against HIV-1. Int. J. Nanomed. 11, 1281–1294.
Yine, H., Shufang, D., Bin, W., Wei, Q., Junling, G., Ashraf, M.A., 2015. Analysis of the relations between allergen specific LgG antibody and allergic dermatosis of 14 kinds foods. Open Med. 10, 405–409.
Wilson, L.J., Yang C, M., Murray, W.V., 2007. Novel cycloalkene indole carbazole alkaloids via the ring closing metathesis reaction. Tetrahedron Lett. 48 (41), 7399–7403.
Worley, B.V., Soto, R.J., Kinsley, P.C., Schoenfisch, M.H., 2016. Active release of nitric oxide-releasing dendrimers from electrospun polyurethane fibers. ACS Biomater. Sci. Eng. 2 (3), 426–437.
Xie, H., Huang, H., He, W., Fu, Z., Luo, C., Ashraf, M.A., 2016. Research on in vitro release of Isoniazid (INH) super paramagnetic microspheres in different magnetic fields. Pak. J. Pharm. Sci. 29 (6), 2207–2212.